A photon counting detector model based on increment matrices to simulate statistically correct CT detector signals

S. Faby[1], J. Maier[1], D. Simons[2], H.-P. Schlemmer[2], M. Lell[3], and M. Kachelrieß[1]

[1]Medical Physics in Radiology, German Cancer Research Center (DKFZ), Heidelberg, Germany
[2]Radiology, German Cancer Research Center (DKFZ), Heidelberg, Germany
[3]Department of Radiology, Friedrich-Alexander-University (FAU), Erlangen, Germany

GERMAN CANCER RESEARCH CENTER IN THE HELMHOLTZ ASSOCIATION

50 Years – Research for A Life Without Cancer

sebastian.faby@dkfz.de

Introduction

Energy-selective photon counting (PC) detectors based on CdTe semiconductor sensors are of increasing interest in the medical community amongst others due to their promising CNR enhancing and material decomposition capabilities. While ideal PC detectors would offer dose saving potential compared to today's dual energy CT, in practice they perform worse. Different processes in the sensor lead to energy dispersion and incomplete charge collection (Fig. 1). These effects do not only affect the spectral response, but also lead to correlations between neighboring pixels and their different energy bins. During image reconstruction the correlations between the energy bins of neighboring pixels can cause correlations between the energy bin images. Correlations between energy bin images can improve the material decomposition performance compared to uncorrelated images. To realistically assess the performance of PC detectors, it is necessary to consider the correct statistical properties of the counting data. The aim of this work is to set up a PC detector model that is easy and fast to use and able to provide statistically correct data. There are many different approaches to model a PC detector, e.g. Monte Carlo simulations or cascaded system models. We introduce in this work a novel increment matrix concept representing the correlations between neighboring pixels and their energy bins.

Materials and Methods

Increment matrices describe the energy bin counter increases resulting from a particular single photon event in all energy bins of a $K \times K$ neighborhood using binary matrices, containing either 0 or 1. Since every energy bin b requires its own increment matrix $I(u,v)$, this stack of matrices is referred to as increment matrix set $I^b(u,v)$. An example for these increment matrix sets for K=3 for a two energy bin system can be found in Figs 2 and 3. The calculation of the detector signal based on the increment matrix sets is explained in Fig. 4. The difficult part is to obtain the probabilities $P(n,E)$. This has to be done only once for a certain detector. The idea is to generate this information and store it for later use. The probabilities corresponding to the different increment matrix sets are obtained by simulating all kinds of photon events in a single detector pixel and by determining the resulting counter increases in all detector pixels in the $K \times K$ neighborhood.

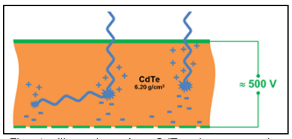

Fig. 1: Illustration of a CdTe photon counting detector showing incident x-ray photons and the resulting electron-hole-pairs. The x-ray photon on the left creates a secondary event (fluorescence photon or Compton scattering). These effects together with the charge cloud drift lead to energy dispersion and a reduced detector performance.

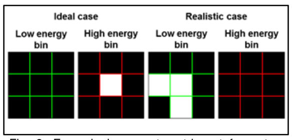

Fig. 2: Example increment matrix set for a two energy bin system in an ideal (left) and a realistic case (right). It illustrates the detector response and the correct correlations resulting from a single photon incident off-center on the central pixel (black=0, white=1). The green and red lines separate the detector pixels only visually.

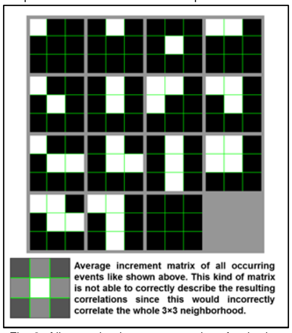

Fig. 3: All occurring increment matrices for the low energy bin. A maximum of four simultaneous counter increases is observed. Matrices that can be generated by symmetry operations from the ones above are not explicitly shown.

The number of photons $N(n,u,v)$ interacting with the detector via increment matrix set n is given by the probability $P(n,E)$ for increment matrix set n to occur with an incident photon of energy E, the detector absorption efficiency $\eta(E)$ and the photon spectrum $N(E,u,v)$:

$$N(n,u,v) = \sum_E P(n,E)\eta(E)N(E,u,v)$$

The photon number $N(n,u,v)$ is the expected value of a Poisson distribution and its noisy realization is indicated by ~. The statistically correct detector signal $S_b(u,v)$ in energy bin b is obtained by a convolution of $N(n,u,v)$ with the increment matrix sets $I^b_n(u,v)$:

$$\tilde{S}_b(u,v) = \sum_n I^b_n(u,v) * \tilde{N}(n,u,v)$$

Poisson noise should not be added directly to $S_b(u,v)$ since this would neglect all correlations and give incorrect statistics.

Fig. 4: Description of the noisy detector signal generation employing the novel increment matrix concept.

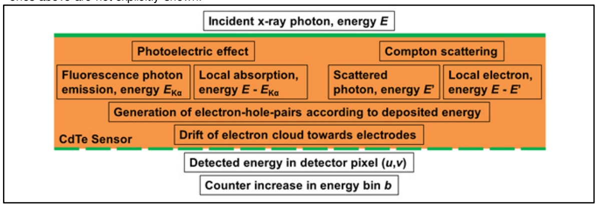

Fig. 5: Overview of the simulated physical processes in the semiconductor sensor. For simplicity multiple scattering is neglected and all secondary photons are assumed to be completely absorbed at their second point of interaction, which is defined by the mean free path in CdTe corresponding to the photon energy.

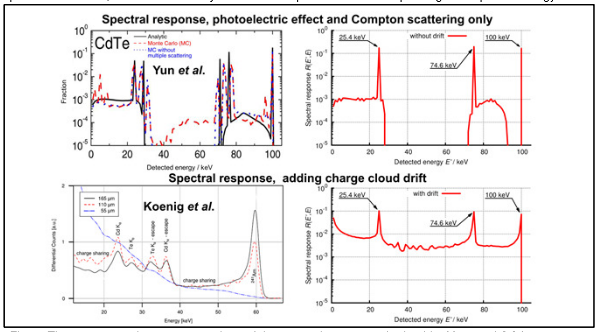

Fig. 6: The upper row shows a comparison of the spectral response obtained by Yun *et al.* [1] for a 0.5 mm thick CdTe sensor with 100 µm pixel size for 100 keV incident photons with the one from our model. The results are based only on the photoelectric effect and Compton scattering (neglecting multiple scattering). The differences between the two models result from the fact that Yun *et al.* derived the spectral response analytically, whereas our model uses a discrete sampling of secondary photon emission.
The lower row illustrates the effect of the charge cloud drift on the spectral response (bias voltage 500 V). The measured results from Koenig *et al.* [4] on the left indicate that the charge sharing background is in reality much more prominent at a significant fraction of the photopeak height and that it extends over the full energy range below the photopeak. The results from our model including the charge cloud drift simulation are shown on the right and stress the influence of the charge cloud broadening on the spectral response.

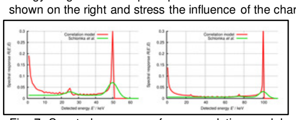

Fig. 7: Spectral response of our correlation model and the parameterized model of Schlomka *et al.* [5] for 50 keV (left) and 100 keV (right) (400 µm pixels, 3 mm CdTe, 500 V).

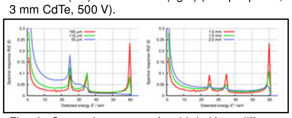

Fig. 8: Spectral response for 60 keV at different pixel sizes (1 mm CdTe, bias voltage 400 V) (left, compare to results of Koenig *et al.* in Fig. 6). Influence of the sensor thickness for the same scenario at 165 µm pixel size (right).

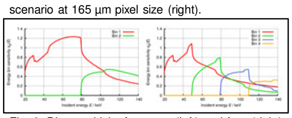

Fig. 9: Bin sensitivity for a two (left) and four (right) bin system (225 µm pixels, 1.6 mm CdTe, 500 V).

Measurement of the covariance matrix of the reconstructed low and high energy bin image using the correlation model. The left matrix shows the results for adding the noise to $S_b(u,v)$. The right matrix shows the results for noise added to $N(n,u,v)$. 50 independent noise realizations have been used.

Covariance matrix no correlations

	Bin 1	Bin 2
Bin 1	113.0%	0.1%
Bin 2	0.1%	268.8%

Covariance matrix correlations

	Bin 1	Bin 2
Bin 1	100.0%	-2.5%
Bin 2	-2.5%	268.3%

If noise is added to $S_b(u,v)$, there are no correlations and the variance in the energy bin images is not correct. Adding noise to $N(n,u,v)$ leads to statistically correct signals and correlations between the energy bins.

Bin 1 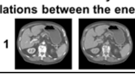 **Bin 2**

Fig. 10: The influence of the correlation model on the covariance matrix of two reconstructed energy bin images (bin 1: 20-80 keV, bin 2: 80-140 keV). The detector was simulated using 225 µm pixels, 1.6 mm thick CdTe and a bias voltage of 500 V.

The signal generation in the sensor during the simulation of photon events is divided into two parts. The first part describes the photon-matter-interaction based on the photoelectric effect (with either K_α-fluorescence photon emission or Auger effect) and Compton scattering. This includes sampling the directions of the emitted or scattered secondary photons. The probability for a certain type of event can be derived from tabulated values and analytical formulas [1]. We neglect multiple scattering, assuming all secondary photons to be absorbed at the second point of interaction given by the mean free path in CdTe for the photon energy. Additionally, the CdTe compound semiconductor is assumed to emit only fluorescence photons with an average energy of the one of Cd and Te since the two K_α-energies are only about 4 keV apart. The second part of the signal generation is concerning the drift of the electron charge cloud, simulating charge sharing. The drift modeling includes cloud broadening due to diffusion and Coulomb expansion [2,3]. The charge density is represented by a Gaussian distribution with a time-dependent standard deviation. Integrating the charge density over the volume of each pixel of the $K \times K$ neighborhood yields the detected energy in this pixel. The detected energy is then compared to the thresholds to determine the resulting counter increases. An overview of the simulated processes and the signal generation is shown in Fig. 5.

Results

Results of our correlation model are presented in Figs 6-10. Fig. 6 emphasizes the importance of the charge cloud drift simulation. Figs 7 and 8 show spectral response functions for different scenarios. Our model is found to yield a good agreement to other models and measurements. In Fig. 9 energy bin sensitivity functions are plotted for a two and a four bin system. The results in Fig. 10 show that correlations between energy bins of neighboring pixels indeed cause correlations between energy bin images.

Acknowledgments

This work was supported by the Deutsche Forschungsgemeinschaft (DFG) under grant KA 1678/5-1 and LE 2763/1, and by the German Government, Bundesministerium für Bildung und Forschung (01EX1012B, Spitzencluster Medical Valley). Parts of the reconstruction software were provided by RayConStruct® GmbH, Nürnberg, Germany.

[1] Yun, S., Kim, H. K., Youn, H., Tanguay, J., and Cunningham, I. A., "Analytic model of energy-absorption response functions in compound x-ray detector materials," IEEE TMI 32, 1819–1828 (2013).
[2] Gatti, E., Longoni, A., Rehak, P., and Sampietro, M., "Dynamics of electrons in drift detectors," NIM Phys Res A 253(3), 393–399 (1987).
[3] Rykov, V. L., Bellwied, R., French, A., Hall, J. R., Pruneau, C., and Wilson, W. K., "SSD signal parametrization," STAR Note 170, 1–22 (1994).
[4] Koenig, T., Schulze, J., Zuber, M., Rink, K., Butzer, J., Hamann, E., Cecilia, A., Zwerger, A., Fauler, A., Fiederle, M., and Oelfke, U., "Imaging properties of small-pixel spectroscopic x-ray detectors based on cadmium telluride sensors," PMB 57, 6743–6759 (2012).
[5] Schlomka, J. P., Roessl, E., Dorscheid, R., Dill, S., Martens, G., Istel, T., Bäumer, C., Herrmann, C., Steadman, R., Zeitler, G., Livne, A., and Proksa, R., "Experimental feasibility of multi-energy photon-counting K-edge imaging in pre-clinical computed tomography," PMB 53(15), 4031–4047 (2008).